# NOTICE CONCERNING COPYRIGHT RESTRICTIONS

# Prediction of Seismic Observables from Geothermal Reservoir Simulations

**Jeffry L. Stevens[1], John W. Pritchett[1], Sabodh K. Garg[1], Tsuneo Ishido[2], and Toshiyuki Tosha[2]**

**[1]Science Applications International Corporation**
**10260 Campus Point Drive, MS X1, San Diego, CA 92121, USA**
**[2]Institute for Geo-Resources and Environment,**
**Geological Survey of Japan/AIST, Central 7, Tsukuba, 305-8567, Japan**

***Keywords***

*Seismic, reservoir simulation, VSP, reflection seismology, crosshole tomography*

## ABSTRACT

We have developed a seismic postprocessor for use in connection with numerical geothermal reservoir simulations. The seismic postprocessor is designed to predict temporal changes in seismic properties and the resulting changes in seismic observables such as travel time, attenuation and reflections that are caused by subsurface changes in the geothermal reservoir. The changes to seismic properties are predicted using Biot theory and empirical relationships. Changes to observables are then predicted by calculating the propagation of seismic waves through this structure. Since the geothermal simulation is in general performed on a coarse grid relative to the resolution required for seismic simulations, an interpolation scheme is developed to optimize prediction of observables and avoid artifacts induced by the coarseness of the geothermal grid. The seismic postprocessor can be used to predict the results of passive seismic surveys, reflection surveys, VSP surveys, and crosshole tomography surveys.

## Introduction

Production of energy from geothermal reservoirs causes changes to the subsurface seismic velocity structure, which may be observable through a variety of types of seismic surveys. These seismic surveys can therefore be used to understand the properties of the reservoir. Of particular interest is using seismic surveys to understand the changes that occur in a geothermal field as the field is produced. In this paper, we describe a seismic modeling technique that can be used together with a geothermal reservoir simulator to predict seismic observables over the lifetime of the field. Some of this work was discussed previously by Stevens *et al.* (2000).

## Estimation of Reservoir Seismic Properties

Geothermal reservoir simulations yield temperature, gas and water content over a three-dimensional grid for a range of time intervals. Typically zero time corresponds to the state of the field in its "natural state" prior to start of production or injection, and calculations may simulate the entire lifetime of the reservoir (~30 years or more). The quantities computed by the reservoir model that are relevant to the seismic calculation are temperature, porosity, water saturation, steam saturation, rock density, and temperature-dependent water and steam density.

The seismic velocity model is not part of the geothermal reservoir calculation, so velocities must be estimated or constrained by other information. Changes in rock density are usually not considered in reservoir simulations. The seismic velocity model is constructed as follows. First, we use parameters for rock velocity and density that are consistent with our experience in geothermal fields, or, if available, from core samples for a specific field; second, we use empirical relations to derive related quantities; and third, we use Biot theory to calculate the mixed phase (rock/water/steam) velocity.

We start by estimating the rock grain velocity $V_r$ using either core samples or typical velocities obtained from the literature. Porous rock is more compliant and therefore has a lower velocity than the rock grains themselves. If not known, the rock density $\rho_r$ is estimated from the velocities $V_r$ using Gardner's relation (Gardner *et al.*, 1974; Sheriff and Geldart, 1983): $\rho_r = 310\, V_r^{1/4}$ (with $\rho_r$ in kg/m$^3$ and $V_r$ in m/s). Based on typical values of rock moduli from geothermal fields, we set the grain bulk modulus to $K_r = 0.9\,\rho_r V_r^2$, the bulk modulus of porous rock $K_p = K_r/4$, and set the shear modulus of the porous rock $\mu = K_r/6$. Velocity also decreases with increasing temperature. Based on data for dry sandstone in Gregory (1977), we model the temperature effect by reducing the elastic moduli by 7% per 100°C, which corresponds to a velocity decrease of about 3% per 100°C.

Biot theory (Gregory, 1977; Garg and Nayfeh, 1986) is used to calculate the velocities of the liquid/solid/gas mixture. To a

very good approximation, if the gas (steam) content is nonzero, then the rock/fluid mixture bulk modulus $K_m$ is equal to $K_p$. If the steam content is zero, then the following relation holds ($K_f$ is the fluid bulk modulus):

$$K_m = K_p + \left(1 - \frac{K_p}{K_r}\right)^2 \left\{\frac{\varphi}{K_f} + \frac{(1-\varphi)}{K_r} - \frac{K_p}{K_r^2}\right\}^{-1}$$

where $\varphi$ is the porosity. The density $\rho_m$ of the water/gas filled rock is given by:

$$\rho_m = (1-\varphi)\rho_r + \varphi(1-S)\rho_f + \varphi S\rho_g$$

where $\rho_f$ is the fluid density, $\rho_g$ is the gas density, and $S$ is the steam saturation. The porous velocity $V_p$ is then given by

$$V_p = \left[\frac{(K_m + 4/3\mu)}{\rho_m}\right]^{1/2}$$

In the following sections, we discuss an example, using a reservoir simulation for a typical geothermal field (after Pritchett *et al.* (2000), grid shown in Figure 1). We use the following properties to calculate the velocity field and seismic observables. Since velocity generally increases with depth, we use a dry rock grain velocity that increases linearly from 4000 m/sec at the surface to 6000 m/sec at a depth of 3 km. This leads to reservoir velocities that range from 2785 m/sec to 4340 m/sec and densities ranging from 2465 kg/m$^3$ to 2728 kg/m$^3$. Regions where steam develops have significantly lower velocities than regions containing no steam, and the region containing steam expands substantially as the reservoir is exploited in the simulation.

## Interpolation to Seismic Grid

As can be seen from Figure 1, the geothermal calculation is performed using grid blocks with a minimum size of 300 meters in horizontal width and 150 meters vertical thickness. The predicted seismic velocities may vary substantially between blocks. Consequently, a straightforward conversion of the geothermal grid to a seismic grid with the same block sizes results in significant discontinuities at grid block boundaries, which lead to unrealistic artifacts—such as reflections from block boundaries—in prediction of seismic observables. To avoid this problem, we perform a smooth interpolation of the geothermal reservoir grid to a much finer seismic grid. Changes in seismic properties between grid blocks then appear as gradients in the seismic properties rather than sharp, artificial discontinuities.

## Calculation of Travel Times

Travel times are calculated by a straightforward integral of distance divided by velocity between the source and receiver locations. In the examples given in this paper, we use a straight-line path between the source and receiver. We can also calculate travel time changes using a slightly curved (minimum time) path, but because of the coarseness of the geothermal reservoir grid this refinement does not necessarily provide a more realistic result.

## Calculation of Seismic Reflections

A time series that simulates a seismic reflection survey can be calculated by using predicted reflection and transmission coefficients for waves transmitted vertically downward and reflected vertically upward through the medium. The amplitude of a seismic reflection can be calculated as a product of the transmission coefficients for layers beneath the surface, for all layers traversed in both the downward and upward directions, multiplied by the reflection coefficient of the reflecting layer. As discussed above, the "layers" correspond to a fine grid derived from interpolation of the coarse reservoir grid. The travel time of the reflected arrival can be calculated by summing the travel times for the downgoing and upgoing waves through all layers. A realistic seismogram similar to actual observations can be created by summing all of the reflected arrivals at the appropriate arrival times through a

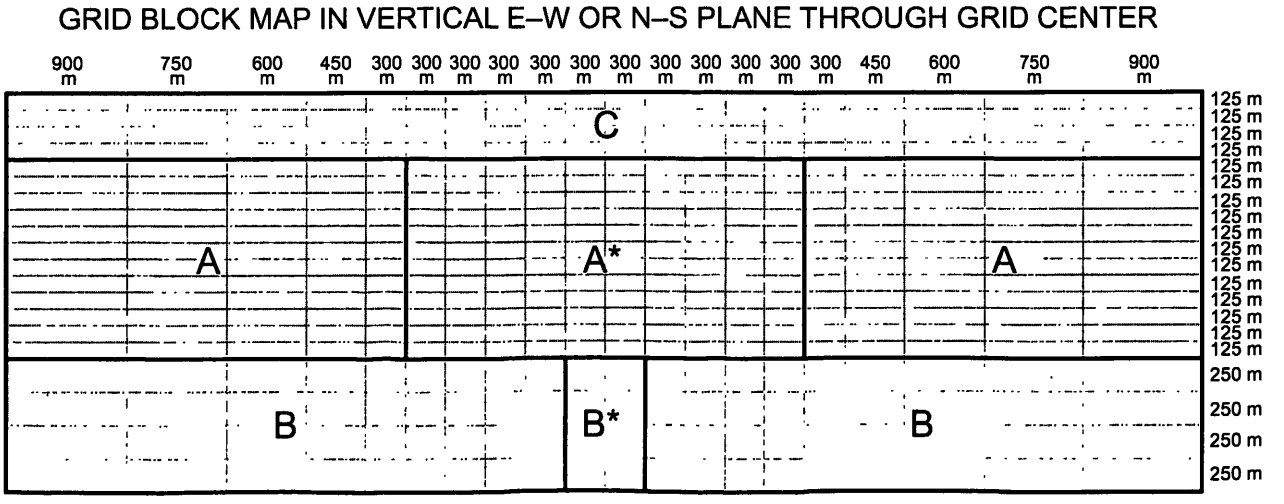


**Figure 1.** Geothermal reservoir simulation of a typical geothermal field from Pritchett et al. (2000). "A" indicates the high-porosity, high-permeability geothermal aquifer. "B" indicates low-porosity basement, which is nearly impermeable except for the region marked "B*" which is permeable and admits incoming hot recharge water from below. "C" indicates high porosity but low permeability caprock.

large number of fine layers, and then filtering the data through a passband similar to those of reflection surveys.

## Calculation of Attenuation

Regions containing a mixture of steam and water are also characterized by high P-wave attenuation. Romero *et al.* (1997) studied the variability in attenuation in the region around The Geysers geothermal field in California, and report that in a steam-bearing region the P-wave attenuation $Q_p^{-1}$ is increased much more than the S-wave attenuation $Q_s^{-1}$ compared to surrounding areas. Ito *et al.* (1979) using data on Massilon sandstone from Winkler and Nur (1979) show that the P-wave attenuation $Q_p^{-1}$ is as high as 0.04 for partially saturated rock at pressures typical of geothermal fields. However $Q_p^{-1}$ drops to less that 0.01 for fully saturated rock and as low as 0.002 for dry rock. The S-wave attenuation $Q_s^{-1}$ is as high as 0.02 for both fully saturated and partially saturated rock, but drops to about 0.005 for dry rock. The high P-wave attenuation provides another way of observing regions of steam in a geothermal field. Romero *et al.* (1997) report $Q_p^{-1}$ measurements as high as 0.1 above a background $Q$ level in The Geysers geothermal reservoir. $Q_p^{-1}$ values can be inferred from spectral ratios using both spectral shape and amplitude. For example, spectral ratios of P-waves observed from local earthquakes propagating through the geothermal field can be used to estimate the attenuation of the signals which can then be used to identify areas containing steam.

To estimate the magnitude of this effect, we calculate the attenuation of signals traveling through the geothermal simulation. The amplitude of signals traveling through the structure is given by

$$A = A_0 \, exp\left[-\int \frac{\pi f}{Q_p V_p} dx\right]$$

where $A_0$ is the amplitude at the bottom of the structure and the integral is over the path through the structure, and $f$ is the frequency.

## Model of Passive Seismic Survey

In this and the following examples, we use the geothermal simulation of Pritchett et al (2000) discussed above. A cross-section through the grid is shown in Figure 1, and the top of the grid and regions of production and injection are shown in Figure 2. The calculation is initially run long enough to achieve a stable "natural state" condition, and then run as a producing field for a period of 10,000 days. Snapshots of the field condition are saved at times of 1000, 2000, 5000, and 10,000 days after the start of production.

In a passive seismic survey, seismic waves from earthquakes or other sources are observed as they pass through the region of interest. Differences between these signals are used to infer the properties of the region, and if multiple surveys are taken at different times, changes in the signals can be related to changes in the properties of the region. The changes in travel times of vertically incident waves traveling through the geothermal simulation from the start of production to 1000 days and 10,000 days, respectively, are shown in Figures 3 and 4, overleaf. As can be seen from Figure 3, over the first 1000 days there is a pronounced decrease in velocity and corresponding increase in travel time in the producing region due to increased steam, and an increase in velocity and decrease in travel time in the region of injection due to cooling. After 10,000 days, the velocity has increased throughout most of the field due to cooling after a long period of production, with the cooling most pronounced in the region of injection. The change in attenuation through

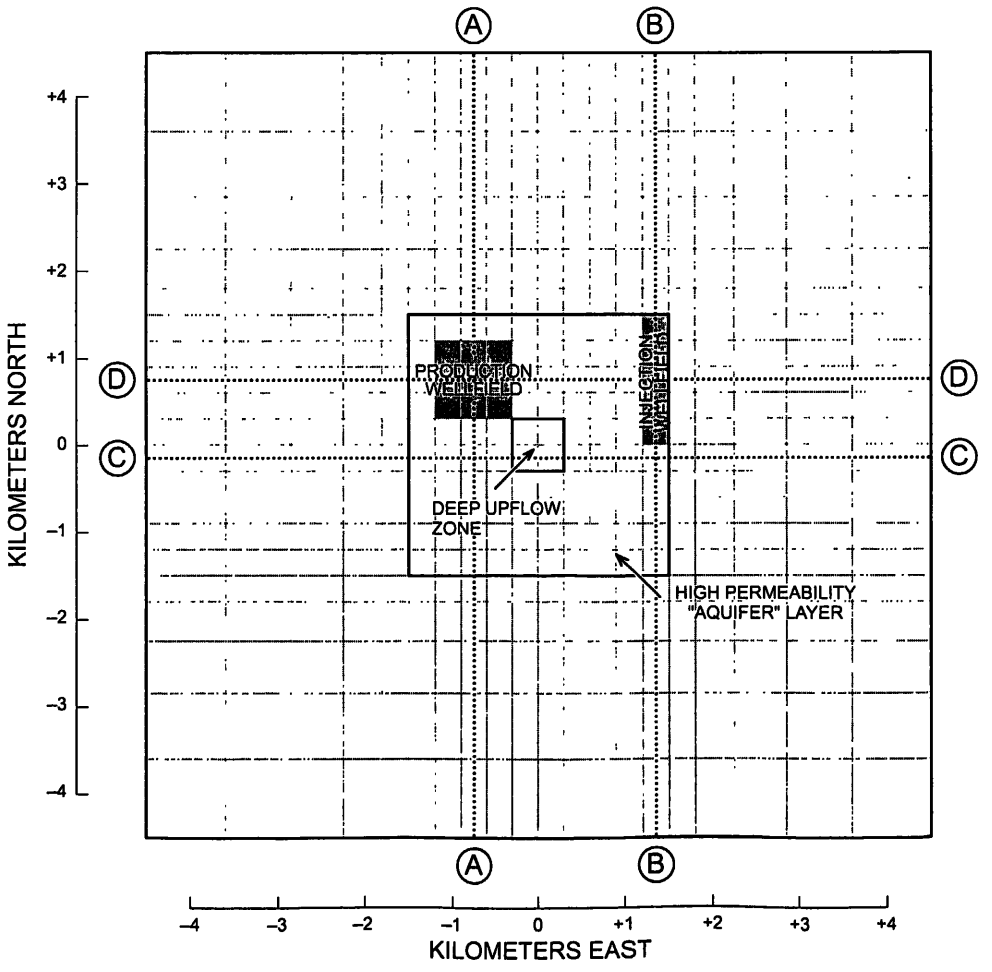


**Figure 2.** Top of the simulator grid area showing regions of production and injection, and area with hot water upflow from depth.

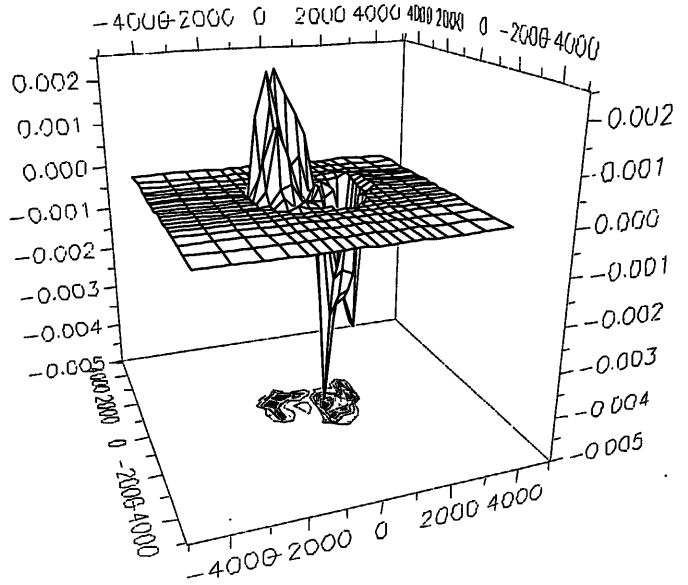


**Figure 3.** Travel time differences between zero and 1,000 days. The travel times increase near the production region due to steam expansion and decrease in the region being cooled by injection. Times shown are in seconds, coordinates are in meters.

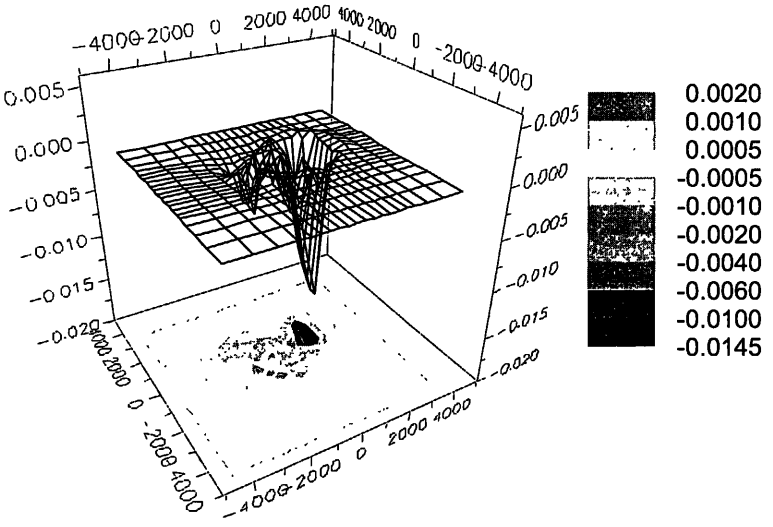


**Figure 4.** Travel time differences between zero and 10,000 days. The deep negative region corresponds to injection, and the high amplitude region corresponds to the edge of the steam zone, which has expanded during this time period.

the field over 10,000 days, which is characterized by increased attenuation in the producing region and decreased attenuation in the injection region, is shown in Figure 5, overleaf. Since the changes in travel time are small, changes in attenuation may be easier to observe.

## Model of Reflection Survey

Seismic reflection surveys use seismic waves generated by artificial sources such as explosions or vibrators on the surface,

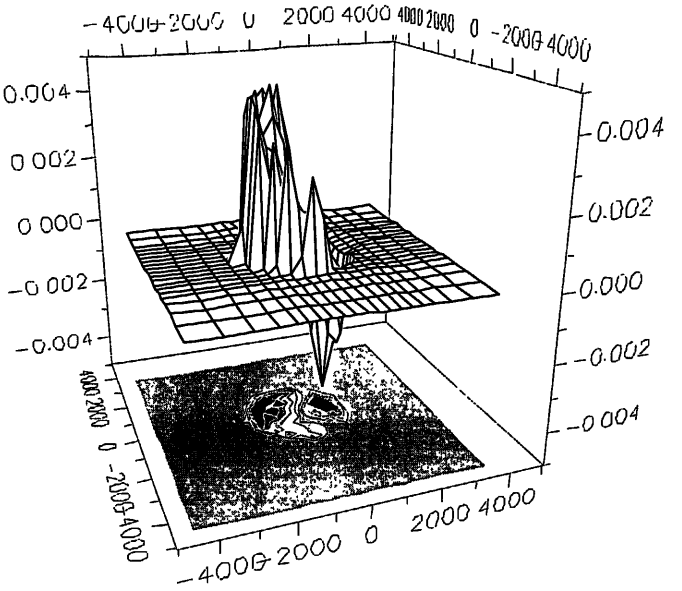


**Figure 5.** Change in log attenuation through the geothermal field after 10,000 days of operation.

and observed as reflected waves. The reflected time series are processed to correspond as much as possible to vertically incident reflected waves. The reflection survey can therefore be simulated as discussed above by calculating the reflections and transmissions of a surface source through the medium and predicting the arrivals at the surface. A predicted east-west reflection survey across the center of the grid area when the field is in its natural state is shown in Figure 6. A corresponding predicted reflection survey across the center of the grid after 10,000 days of production is shown in Figure 7. Note the differences in character of the reflected waves, particularly the stronger reflections in regions containing steam, and the apparent "movement" of the basement location caused be changes in velocity above the basement.

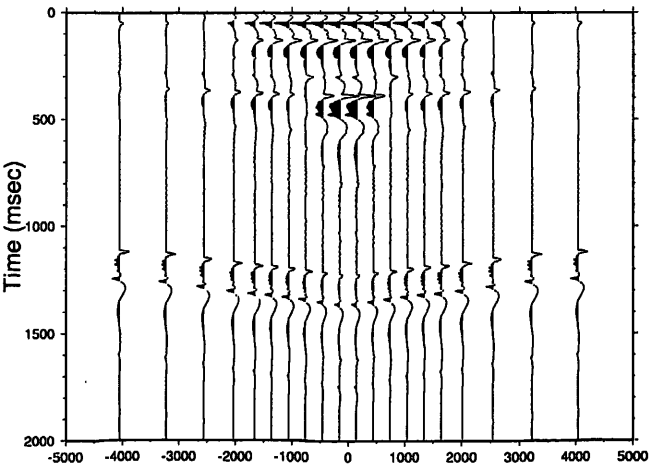


**Figure 6.** East-west seismic section across the center of the calculated region in the natural state.

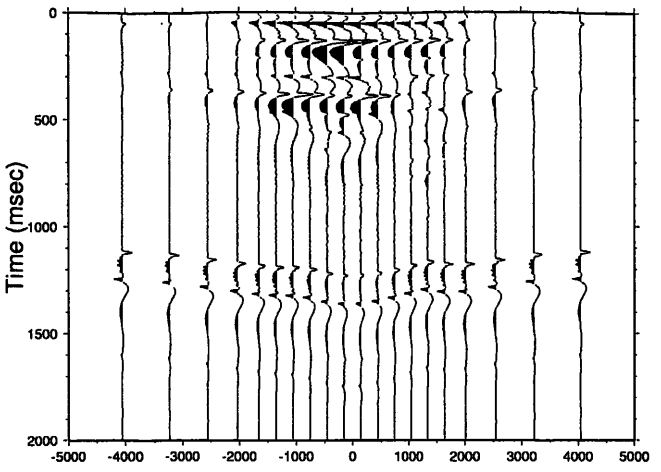


**Figure 7.** East-west seismic section across the center of the calculated region after 10,000 days of production.

## Model of Crosshole Survey

A crosshole survey uses travel times from a set of sources in one borehole to a set of receivers in another to infer the seismic velocities of the region between the boreholes. We calculate the travel times for rays between two hypothetical wells at the outer boundaries of the producing region (along path A-A of Figure 2). These simulate a crosshole experiment between two wells separated by 900 meters, with surveys performed both 0 and 10,000 days after the start of production. The simulation uses 25 sources and 25 receivers evenly spaced at 50-meter intervals from depths of 50 meters to 1250 meters. The crosshole travel time from a source at 550 meters depth to receivers in the second borehole for the field in its natural state and after 10,000 days of production are shown in Figure 8. The travel times change substantially due to production, particularly in the region between 400 and 700 meters depth.

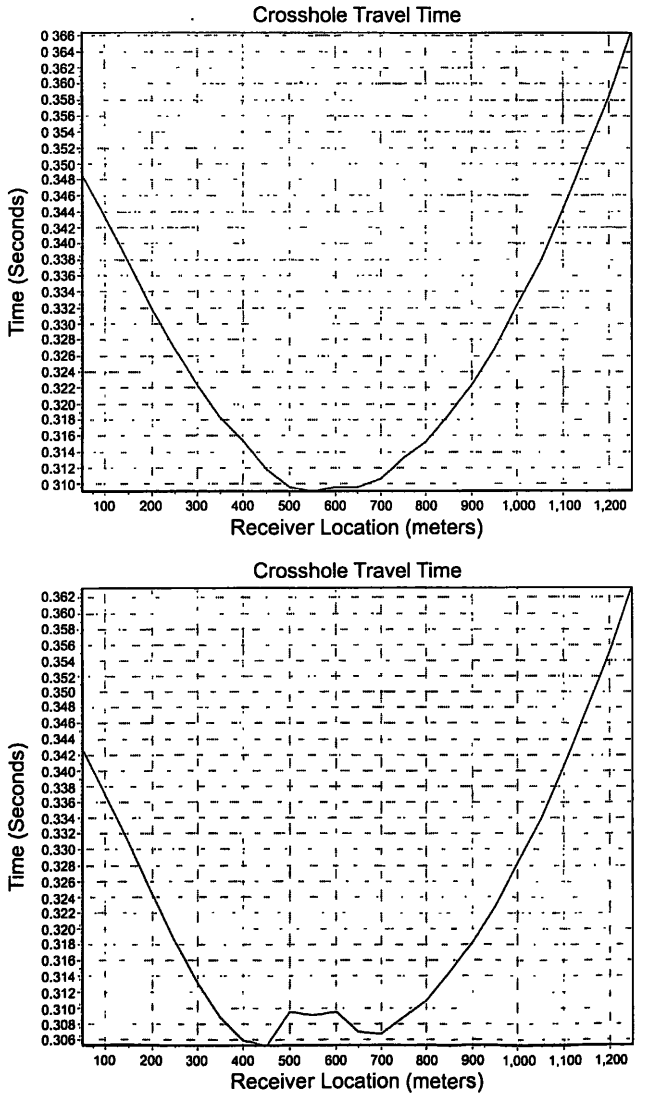


**Figure 8.** Crosshole travel time from a source at 550 meters depth to receivers at depths ranging from 50 to 1250 meters for the field in its natural state (top) and after 10,000 days of production (bottom).

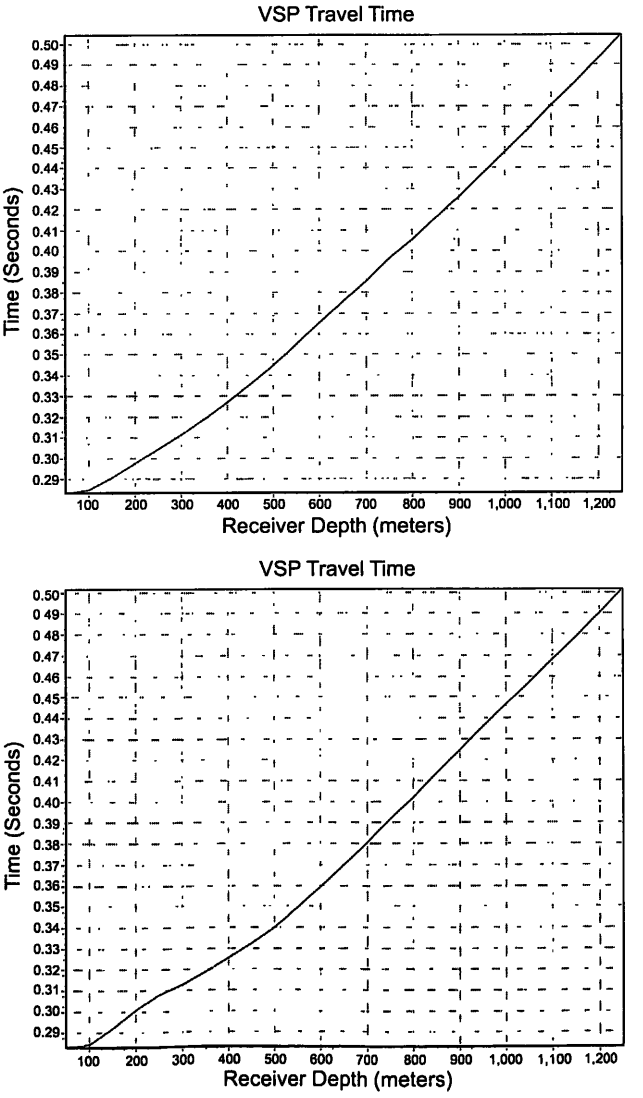


**Figure 9.** Travel times from a VSP survey for a source at one end of the producing region to a borehole on the other end for the field in its natural state (top) and after 10,000 days of production (bottom).

## Model of Vertical Seismic Profile Survey

Vertical Seismic Profiling (VSP) is similar in many respects to a crosshole survey. In a typical VSP survey, a recording instrument or instruments are placed deep in a borehole, and a source generates seismic waves at one or more locations on the surface or in a nearby shallow borehole. The arrival time of the signal is measured and used to infer the velocity structure between the source and receiver. In our example, sources are at the surface crossing the producing region of the field, and the receiving well is at the northern boundary of the producing region. Sources are spaced 50 meters apart over a distance of 1 km, and receivers are spaced at 50-meter intervals between 50 meters and 1250 meters depth. The predicted travel times from a source across the producing region from the well containing the receivers are shown in Figure 9. The travel times for the natural state are shown in the top figure and the travel times after 10,000 days of production are shown in the bottom figure.

## Conclusions

We have developed a seismic postprocessor for geothermal reservoir simulations capable of modeling passive seismic surveys, reflection surveys, crosshole surveys and VSP surveys, and performed sample calculations for a simulated typical geothermal reservoir. The postprocessor is useful for predicting the nature and magnitude of changes that would be expected for a geothermal field over its lifetime. These results can in turn be used as a guide for performing each type of seismic survey for monitoring of a geothermal field.

## References

Gardner, G. H. F., Gardner, L. W., and Gregory, A. R. (1974), "Formation velocity and density – the diagnostic basics for stratigraphic traps," *Geophysics*, 16, pp. 673-685.

Garg, S. K. and A. H. Nayfeh (1986), "Compressional wave propagation in liquid and/or gas saturated elastic porous media," *J. Appl. Phys.*, 60, pp. 3045-3055.

Gregory, A. R. (1977), "Aspects of rock physics from laboratory and log data that are important to seismic interpretation," in *Seismic Stratigraphy – Applications to Hydrocarbon Exploration*, pp. 15-46 (ed. C. E. Peyton), Tulsa, AAPG Memoir 26.

Ito, H., J. DeVilbiss, and A. Nur (1979), "Compressional and shear waves in saturated rock during water-steam transition," *J. Geophys. Res.*, 84, pp. 4371-4735.

Pritchett, J., J. L. Stevens, P. Wannamaker, S. Nakanishi, and S. Yamazawa (2000), "Theoretical Feasibility Studies of Reservoir Monitoring Using Geophysical Survey Techniques," *Proc. World Geothermal Congress 2000*, Japan.

Romero, A. E., T. V. McEvilly, and E. L. Majer (1997), "3-D microearthquake attenuation tomography at the Northwest Geysers geothermal region, California," *Geophysics*, 62, pp. 149-167.

Sheriff, R. E. and L. P. Geldart (1983), *Exploration Seismology, Volume 2: Data Processing and Interpretation*, Cambridge University Press, New York.

Stevens, J. L., J. W. Pritchett, S. K. Garg, K. Ariki, S. Nakanishi, and S. Yamazawa (2000), "Seismic Methods for Observing Geothermal Field Evolution," *Proc. World Geothermal Congress 2000*, Japan.

Winkler, K. and A. Nur (1979), "Pore fluids and seismic attenuation in rocks," *Geophys. Res. Lett.*, 6, pp. 1-4.